

Adaptive Wave Filtering for Dynamic Positioning of Marine Vessels using Maximum Likelihood Identification: Theory and Experiments^{*}

Vahid Hassani^{*} Asgeir J. Sørensen^{**} António M. Pascoal^{***}

^{*} Norwegian Marine Technology Research Institute (MARINTEK), Trondheim, Norway (e-mail: vahid.hassani@marintek.sintef.no)

^{**} Centre for Autonomous Marine Operations and Systems (AMOS) and Dept. of Marine Technology, Norwegian Univ. of Science and Technology, Trondheim, Norway (e-mail: asgeir.sorensen@ntnu.no)

^{***} Laboratory of Robotics and Systems in Engineering and Science (LARSyS), Instituto Superior Técnico (IST), Technical University of Lisbon, Portugal; Adjunct Scientist with the National Institute of Oceanography (NIO), Goa, India (e-mail: antonio@isr.ist.utl.pt)

Abstract: This paper addresses a filtering problem that arises in the design of dynamic positioning systems for ships and offshore rigs subjected to the influence of sea waves. The dynamic model of the vessel captures explicitly the sea state as an uncertain parameter. The proposed adaptive wave filter borrows from maximum likelihood identification techniques. The general form of the logarithmic likelihood function is derived and the dominant wave frequency (the uncertain parameter) is identified by maximizing this function. To this effect, a bank of Kalman filters is used to evaluate the log-likelihood function for different values of the uncertain parameter. After each identification step a new set of Kalman filters is designed to estimate the dominant wave frequency with better accuracy. The proposed sea state identification technique enables adaptive Wave Filtering (WF) and Dynamic Positioning (DP) systems to operate in different operational conditions and hence, it is a step forward to the development of a so-called all-year marine estimation and control system. The results are experimentally verified by model testing a DP operated ship, the Cybership III, under different sea conditions in a towing tank equipped with a hydraulic wave maker.

Keywords: Adaptive wave filtering, dynamic positioning, marine vessels, maximum likelihood identification.

1. INTRODUCTION

The advent of offshore exploration and exploitation at an unprecedented scale has brought about increasing interest in the development of Dynamic Positioning (DP) systems for surface vessels. For this reason, the number of vessels whose position is regulated by means of DP systems has significantly increased during the last decades. In deep waters, Jack-up barges and anchoring systems cannot be used economically and DP systems are needed to keep the position and heading of marine structures within pre-specified excursion limits under expected weather windows. Early DP systems were implemented using PID controllers. In order to restrain thruster trembling caused by the wave-induced motion components, notch filters in cascade with low pass filters were used with the controllers. However, notch filters restrict the performance of closed-loop systems because they introduce phase lag around the crossover frequency, which in turn tends to decrease phase margin. An improvement in performance was achieved

^{*} This work was supported in part by projects MORPH (EU FP7 under grant agreement No. 288704) and the FCT [PEst-OE/EEI/LA0009/2011] and was carried cooperatively by the Norwegian Marine Technology Research Institute (MARINTEK), LARSyS-Instituto Superior Técnico (IST), Technical University of Lisbon, Portugal, and the Centre for Autonomous Marine Operations and Systems (AMOS); the Norwegian research council is acknowledged as sponsor of MARINTEK and AMOS.

by exploiting more advanced control techniques based on optimal control and Kalman filter (KF) theory, see Balchen et al. (1976). These techniques were later modified and extended in Sælid et al. (1983); Sørensen et al. (1996); Grøvlen and Fossen (1996); Torsetnes et al. (2004); Nguyen et al. (2007); Hassani et al. (2012), and Hassani et al. (2013c). For a survey of dynamic positioning control systems, see Hassani et al. (2012, 2013c), and Sørensen (2011) and the references therein. One of the most fruitful concepts introduced in the course of the body of work referred above was that of wave filtering, together with the strategy of modeling the total vessel motion as the superposition of low-frequency vessel motion and wave-frequency motions. It was further recognized that in order to reduce the mechanical wear and tear of the propulsion system components, in small to high sea states, the estimates entering the DP control feedback loop should be filtered by using a so-called wave filtering technique so as to prevent excessive control activity in response to wave frequency components. Furthermore, only the slowly-varying disturbances should be counterbalanced by the propulsion system, whereas the oscillatory motion induced by the waves (1st-order wave induced loads) should not enter the feedback control loop. To this effect, DP control systems should be designed so as to react to the low frequency forces on the vessel only. In practice, position and heading measurements are corrupted not only by sensor

noise but also by colored noise caused by wind, waves, and ocean currents. In addition, in general measurements of the vessel's velocity are not available; thus the need for an observer to estimate the vessel's velocity from corrupted measurements of position and heading and achieve wave filtering while "separating" the low-frequency and wave-frequency position and heading estimates (see Fossen (2011) for details).

In Sørensen et al. (1996), Wave Filtering (WF) was done by exploiting the use of KF theory under the assumption that the kinematic equations of the ship's motion can be linearized about a set of predefined constant yaw angles (36 operating points in steps of 10 degrees, covering the whole heading envelope); this is necessary when applying linear KF theory and gain scheduling techniques. However, global exponential stability (GES) of the complete system cannot be guaranteed. In Fossen and Strand (1999), a nonlinear observer with wave filtering capabilities and bias estimation was designed using passivity. The sea state may undergo large variations and therefore the observer in charge of reconstructing the LF motion should adapt to the sea state itself; adaptive WF and DP were introduced in Strand and Fossen (1999); Torsetnes et al. (2004); Nguyen et al. (2007); Hassani et al. (2012, 2013c), and Sørensen (2011), where adaptation to sea state change was introduced.

In this paper, inspired by previous pioneering work on DP Systems, a modified model for wave filtering, proposed in Hassani et al. (2012) is used. Based on the adopted model, we propose the use of an adaptive wave filter coupled with a maximum likelihood parameter identification technique. To this effect, the log-likelihood function is defined and a bank of KFs based on some initial values for the uncertain parameter is formed; the log-likelihood function (as a performance index for WF) is evaluated for the nominal parameter set. Maximization of the log-likelihood function over the nominal uncertain parameters is studied and a new set of KFs are designed and exploited to further refine the estimates of the uncertain parameter. At each stage the estimated dominant wave frequency is used to identify the sea condition, based on which adaptive wave filtering, using Kalman filtering, is performed for dynamic positioning systems. The main emphasis of the paper is on the use of maximum likelihood parameter identification techniques for WF; however, for the sake of completeness, the relation between the proposed methodology and Multiple Model Adaptive Wave filtering, MMA-WF (see Hassani et al. (2012), and Hassani et al. (2013c)) is studied.

The structure of the paper is as follows. Section 2 proposes a linear representative vessel model. Section 3 describes the key idea behind the proposed parameter identification technique. It also provides a summary of Maximum likelihood parameter identification and studies the similarities and differences of the proposed algorithm and MMA-WF. In section 4, a short description of the model test vessel, Cybership III, and experimental results of model tests are presented. Conclusions and suggestions for future research are summarized in Section 5.

2. LINEAR MODEL OF THE DP VESSEL

In what follows, a vessel model that is by now standard¹ is presented. See for example Strand and Fossen (1999);

¹ The model described by (1)-(6) has minor differences with respect to the ones normally available in the literature. While in most of the literature the WF components of motion are modeled in a fixed-earth frame, in this paper the WF motion is modeled in body-

Hassani et al. (2012, 2013c). The model admits the realization

$$\dot{\xi}_W = A_W(\omega)\xi_W + E_W w_W \quad (1)$$

$$\eta_W = R(\psi_L)C_W\xi_W \quad (2)$$

$$\dot{b} = -T^{-1}b + E_b w_b \quad (3)$$

$$\dot{\eta}_L = R(\psi_L)\nu \quad (4)$$

$$M\dot{\nu} + D\nu = \tau + R^T(\psi_{tot})b \quad (5)$$

$$\eta_{tot} = \eta_L + \eta_W \quad (6)$$

$$\eta_y = \eta_{tot} + v, \quad (7)$$

where (1) and (2) capture the 1st-order wave induced motions in surge, sway, and yaw; equation (3) represents the 1st-order Markov process approximating the unmodelled dynamics and the slowly varying environmental forces (in surge and sway) and torques (in yaw) due to waves (2nd order wave induced loads), wind, and currents. The latter are given in earth fixed coordinates but expressed in body-axis. In the above, $\eta_W \in \mathbb{R}^3$ is the vessel's WF motion due to 1st-order wave-induced disturbances, consisting of WF position (x_W, y_W) and WF heading ψ_W of the vessel; $w_W \in \mathbb{R}^3$ and $w_b \in \mathbb{R}^3$ are zero mean Gaussian white noise vectors, and

$$A_W = \begin{bmatrix} 0_{3 \times 3} & I_{3 \times 3} \\ -\Omega_{3 \times 3} & -\Lambda_{3 \times 3} \end{bmatrix}, \quad E_W = \begin{bmatrix} 0_{3 \times 1} \\ I_{3 \times 1} \end{bmatrix},$$

$$C_W = [0_{3 \times 3} \quad I_{3 \times 3}],$$

with

$$\Omega = \text{diag}\{\omega_1^2, \omega_2^2, \omega_3^2\},$$

$$\Lambda = \text{diag}\{2\zeta_1\omega_1, 2\zeta_2\omega_2, 2\zeta_3\omega_3\},$$

where $\omega = [\omega_1 \ \omega_2 \ \omega_3]^T$ and ζ_i are the Dominant Wave Frequency (DWF) and relative damping ratio, respectively. Matrix $T = \text{diag}(T_x, T_y, T_\psi)$ is a diagonal matrix of positive bias time constants and $E_b \in \mathbb{R}^{3 \times 3}$ is a diagonal scaling matrix. Vector $\eta_L \in \mathbb{R}^3$ consists of low frequency (LF), earth-fixed position (x_L, y_L) and LF heading ψ_L of the vessel relative to an earth-fixed frame, $\nu \in \mathbb{R}^3$ represents the velocities decomposed in a vessel-fixed reference, and $R(\psi_L)$ is the standard orthogonal yaw angle rotation matrix (see Fossen (2011) for complete details). Equation (5) describes the vessels's LF motion at low speed (see Fossen (2011)), where $M \in \mathbb{R}^{3 \times 3}$ is the generalized system inertia matrix including zero frequency added mass components, $D \in \mathbb{R}^{3 \times 3}$ is the linear damping matrix, and $\tau \in \mathbb{R}^3$ is a control vector of generalized forces generated by the propulsion system, that is, the main propellers aft of the ship and thrusters which can produce surge and sway forces as well as a yaw moment. Vector $\eta_{tot} \in \mathbb{R}^3$ describes the vessel's total motion, consisting of total position (x_{tot}, y_{tot}) and total heading ψ_{tot} of the vessel. Finally, (7) represents the position and heading measurement equation, with $v \in \mathbb{R}^3$ a zero-mean Gaussian white measurement noise.

From (1)-(6), using practical assumptions, a linear model with parametric uncertainty was obtained in Hassani et al. (2012) as follows:

The reader is referred to Hassani et al. (2012) for details and improvements of the present model.

$$\dot{\xi}_W = A_W(\omega)\xi_W + E_W w_W \quad (8)$$

$$\eta_W^b = C_W \xi_W \quad (9)$$

$$\dot{b}^p = -T^{-1}b^p + w_b^f \quad (10)$$

$$\dot{\eta}_L^p = \nu \quad (11)$$

$$M\dot{\nu} + D\nu = \tau + b^p \quad (12)$$

$$\eta_y^f = \eta_L^p + \eta_W^b \quad (13)$$

where η_W^b are WF components of motion on the body-coordinate axis, w_b^f and η_y^f are a new modified disturbance and a modified measurement defined by $w_b^f = R^T(\psi_y)E_b w_b$ and $\eta_y^f = R^T(\psi_y)\eta_y$, respectively, ω , is parametric uncertainty, and matrix S is given by

$$S = \begin{bmatrix} 0 & 1 & 0 \\ -1 & 0 & 0 \\ 0 & 0 & 0 \end{bmatrix}.$$

The equations describing the kinematics and the dynamics of the vessel can be represented in the following standard form for multiple-input-multiple-output (MIMO) linear plant models:

$$\dot{x}(t) = A(\omega)x(t) + Bu(t) + Gw(t), \quad (14a)$$

$$y(t) = Cx(t) + v(t), \quad (14b)$$

where $x(t) = [\xi_W^T \ b^p \ \eta_L^p \ \nu^T]^T \in \mathbb{R}^{15}$ denotes the state of the system, $u(t) = M^{-1}\tau \in \mathbb{R}^3$ its control input, $y(t) = \eta_y^f \in \mathbb{R}^3$ its measured noisy output, $w(t) = [w_W^T \ w_b^f]^T \in \mathbb{R}^6$ an input plant disturbance that cannot be measured, and $v(t) \in \mathbb{R}^3$ is the measurement noise. The equations in (14) are simply a compact way of presenting equations in (8)-(13); $A(\omega)$, B , G , and C are defined in the obvious manner. Table 1 shows the definition of the sea conditions characterized by the DWF. The sea conditions are associated with the particular model of offshore supply vessel that is used in our study. We assume that DWF

Table 1. Definition of Sea States from Price and Bishop (1974)

Sea States	DWF	Significant Wave Height H_s (m)
	ω (rad/s)	
Calm Seas	> 1.11	< 0.1
Moderate Seas	[0.74 1.11]	[0.1 1.69]
High Seas	[0.53 0.74]	[1.69 6.0]
Extreme Seas	< 0.53	> 6.0

lies in the interval $[0.39 \ 1.8]^2$ that covers calm, moderate, high and extreme sea conditions.

3. MAXIMUM LIKELIHOOD PARAMETER IDENTIFICATION

In this section we develop the maximum likelihood function for the discretized model of (15) given by³

$$\begin{aligned} x(t+1) &= A(\theta)x(t) + Bu(t) + G(\theta)w(t), \\ y(t) &= C(\theta)x(t) + v(t). \end{aligned} \quad (15)$$

Let $Y(t) \equiv \{y(0), y(1), \dots, y(t)\}$ express the time history of the observed output. The likelihood of a set of parameter values, θ , given some observed outcomes, $Y(t)$, (denoted by $\mathcal{L}(\theta; Y(t))$) is equal to the probability of those observed

² We use the same interval for DWF in surge, sway and yaw.

³ To consider a more general case we rename the parametric uncertainty by θ and we assume that the parametric uncertainty is present in the A , G , and C matrices.

outcomes assuming that those parameter values were true values in the dynamic of the plant, that is

$$\mathcal{L}(\theta; Y(t)) = p(Y(t); \theta). \quad (16)$$

In other words, the likelihood function of the state space model is a parameterized density function of the set of observations $Y(t)$ which reflects how likely it is to observe $Y(t)$ if θ were the true values of the uncertain parameters.⁴ In fact, $p(Y(t); \theta)$ is a family of density functions that can be computed for different values of θ and observation history $Y(t)$. For a fixed set of observations $Y(t)$, $p(Y(t); \theta)$ is a function of θ and the maximum likelihood estimate $\hat{\theta}$ of θ , is defined as the value that maximizes $p(Y(t); \theta)$ (for the above mentioned fixed $Y(t)$). Using the definition of conditional probability and employing Bayes's theorem recursively, $p(Y(t); \theta)$ can be described as product of conditional densities

$$p(Y(t); \theta) = \prod_{\tau=1}^{\tau=t} p(y(\tau)|Y(\tau-1); \theta). \quad (17)$$

In order to compute $p(y(\tau)|Y(\tau-1); \theta)$ we summarize the classical Kalman filter structure (see Anderson and Moore (1979))

$$\hat{x}_\theta(t+1|t) = A_\theta \hat{x}_\theta(t|t) + Bu(t) \quad (18a)$$

$$\hat{x}_\theta(t|t) = \hat{x}_\theta(t|t-1) + H_\theta(t)(y(t) - \hat{y}_\theta(t|t-1)) \quad (18b)$$

$$\Sigma_\theta(t+1|t) = A_\theta \Sigma_\theta(t|t) A_\theta^T + G_\theta Q G_\theta^T \quad (18c)$$

$$\Sigma_\theta(t|t) = \Sigma_\theta(t|t-1) - H_\theta(t) C_\theta \Sigma_\theta(t|t-1) \quad (18d)$$

$$S_\theta(t) = C_\theta \Sigma_\theta(t|t-1) C_\theta^T + R \quad (18e)$$

$$H_\theta(t) = \Sigma_\theta(t|t-1) C_\theta^T S_\theta^{-1}(t) \quad (18f)$$

$$\hat{y}_\theta(t|t-1) = C_\theta \hat{x}_\theta(t|t-1) \quad (18g)$$

where $[A_\theta, G_\theta]$ and $[A_\theta, C_\theta]$ are assumed to be stabilizable and detectable.

It is well known that in Kalman filtering theory, under the Gaussian assumption, the residuals $\tilde{y}_\theta(t) = y(t) - \hat{y}_\theta(t|t-1)$ form an independent Gaussian sequence such that

$$p(y(t)|Y(t-1); \theta) = \frac{e^{-\frac{1}{2}\tilde{y}_\theta^T(t)S_\theta^{-1}(t)\tilde{y}_\theta(t)}}{(2\pi)^{\frac{q}{2}}\sqrt{|S_\theta(t)|}}, \quad (19)$$

where q is dimension of $y(t)$ and $S_\theta(t)$ is the covariance matrix of residuals in the KF given by (18e).

Combining (19) and (17), under linearity and Gaussian assumptions the likelihood function is given by

$$\mathcal{L}(\theta; Y(t)) = \prod_{\tau=1}^{\tau=t} \frac{e^{-\frac{1}{2}\tilde{y}_\theta^T(\tau)S_\theta^{-1}(\tau)\tilde{y}_\theta(\tau)}}{(2\pi)^{\frac{q}{2}}\sqrt{|S_\theta(\tau)|}}. \quad (20)$$

In practice, it is often more convenient to work with the logarithm of the likelihood function, called the log-likelihood function, defined as

$$\log(\mathcal{L}(\theta; Y(t))) = \quad (21)$$

$$\sum_{\tau=1}^{\tau=t} \left[-\frac{q}{2} \log(2\pi) - \frac{1}{2} \log(|S_\theta(\tau)|) - \frac{1}{2} \tilde{y}_\theta^T(\tau) S_\theta^{-1}(\tau) \tilde{y}_\theta(\tau) \right].$$

The first term on the right hand side of (21) (i.e. $-\frac{tq}{2} \log(2\pi)$) does not depend on θ ; hence, the maximum likelihood estimate $\hat{\theta}$ can be found by maximizing $\sum_{\tau=1}^{\tau=t} [-\frac{1}{2} \log(|S_\theta(\tau)|) - \frac{1}{2} \tilde{y}_\theta^T(\tau) S_\theta^{-1}(\tau) \tilde{y}_\theta(\tau)]$ or by minimizing the "relevant parts" of the negative log likelihood function, denoted by $\mathcal{K}(\theta; Y(t))$, given by

⁴ Strictly speaking, θ is not a random variable and hence, $p(Y(t); \theta)$ is not a conditional density function.

$$\mathcal{K}(\theta; Y(t)) = \sum_{\tau=1}^{\tau=t} \frac{1}{2} [\log(|S_{\theta}(\tau)|) + \tilde{y}_{\theta}^T(\tau) S_{\theta}^{-1}(\tau) \tilde{y}_{\theta}(\tau)]. \quad (22)$$

3.1 Finite Parameter Case

At this stage, let us consider the case where the uncertain parameter θ belongs to a finite set $\Theta = \{\theta_1, \theta_2, \dots, \theta_N\}$. To find the maximum likelihood estimate $\hat{\theta}$, a bank of KFs (with N KFs) can be designed based on models of the plant, taking $\theta_i \in \Theta$ as an uncertain parameter value. At each sampling time, the i^{th} KF in the bank generates $S_{\theta_i}(t)$ and $\tilde{y}_{\theta_i}(t)$ which can be used to evaluate $\mathcal{L}(\theta_i; Y(t))$. Then, the maximum likelihood estimate $\hat{\theta}$ is found as

$$\hat{\theta}(t) = \operatorname{argmax}_{\theta_i \in \Theta} \mathcal{L}(\theta_i; Y(t)). \quad (23)$$

Before considering the compact parameter case, let us take the discussion a stage further and highlight the relations between WF using maximum likelihood identification and Multiple Model Adaptive WF (MMA-WF), see Hassani et al. (2012). In the MMA-WF methodology, a bank of KFs is designed for a finite number of dominant wave frequency values in Θ , each corresponding to a different peak frequency of the assumed wave spectrum model. The a posteriori probability for each KF representing the true model of plant is computed as

$$p_{\theta_i}(t) = \frac{|S_{\theta_i}(t)|^{-\frac{1}{2}} e^{-\frac{1}{2} \tilde{y}_{\theta_i}^T(t) S_{\theta_i}^{-1}(t) \tilde{y}_{\theta_i}(t)}}{\sum_{j=1}^N p_{\theta_j}(t) |S_{\theta_j}(t)|^{-\frac{1}{2}} e^{-\frac{1}{2} \tilde{y}_{\theta_j}^T(t) S_{\theta_j}^{-1}(t) \tilde{y}_{\theta_j}(t)}} p_{\theta_i}(t-1), \quad (24)$$

where $p_i(0)$ are the prior model probabilities. The final parameter estimation can be formed either by the stochastic weighted average

$$\hat{\theta}(t) := \sum_{i=1}^N p_{\theta_i}(t) \theta_i, \quad (25)$$

or by the maximum a posteriori (MAP) estimate

$$\hat{\theta}(t) := \operatorname{argmax}_{\theta_i \in \Theta} p_{\theta_i}(t). \quad (26)$$

Lemma 1. Assuming that the distinguishability condition in Hassani et al. (2009a) and Hassani et al. (2013a) are satisfied, the parameter estimate $\hat{\theta}(t)$ in (23) and (26) coincide. Moreover, the parameter estimate $\hat{\theta}(t)$ in (25) converges to the one in (23) and (26) asymptotically.

Before proving the lemma, let us introduce the Baram index (see Baram and Sandell (1978)) and summarize the main results in Hassani et al. (2009a) and Hassani et al. (2013a). It is shown in Hassani et al. (2009a) and Hassani et al. (2013a) that under some distinguishability conditions, as $t \rightarrow \infty$, one of the posterior probabilities governed by (24) (the a posteriori probability associated with the KF designed based on the closest model to the true plant in a well defined sense), say p_j , converges to 1 and the rest converge to 0. Moreover, it is shown that

$$\Gamma_{\theta_j}^{\theta_*} \leq \Gamma_{\theta_i}^{\theta_*}, \quad \forall \theta_i \in \Theta \quad (27)$$

where $\theta_* \in \Theta$ is the true θ value in the plant and the Baram index denoted by $\Gamma_{\theta_i}^{\theta_*}$ is defined as

$$\Gamma_{\theta_i}^{\theta_*} \equiv +\frac{1}{2} \log(|S_{\theta_i}|) + \frac{1}{2} \operatorname{tr}(S_{\theta_i}^{-1} \mathfrak{S}_{\theta_i}^{\theta_*}), \quad (28)$$

where $\mathfrak{S}_{\theta_i}^{\theta_*}$ is the covariance of the residuals in KF tuned for θ_i while the true parameter in the plant is θ_* and S_{θ_i} denotes $\lim_{t \rightarrow \infty} S_{\theta_i}(t)$.

Proof. To prove the first part of lemma 1 it suffices to show that

$$\operatorname{argmax}_{\theta_i \in \Theta} p_{\theta_i}(t) = \operatorname{argmax}_{\theta_i \in \Theta} \mathcal{L}(\theta_i; Y(t)). \quad (29)$$

It is shown in Hassani et al. (2011) (lemma 1, page 3) that

$$\operatorname{argmax}_{\theta_i \in \Theta} p_{\theta_i}(t) = \operatorname{argmin}_{\theta_i \in \Theta} \mu_{\theta_i}(t), \quad t = 1, 2, \dots \quad (30)$$

where $\mu_{\theta_i}(t)$ are monitoring signals assessing the performance of KFs in the bank and defined as

$$\mu_{\theta_i}(t) = \quad (31)$$

$$\frac{q}{2} \log(2\pi) + \frac{1}{2t} \sum_{\tau=1}^{\tau=t} [\log(|S_{\theta}(\tau)|) + \tilde{y}_{\theta}^T(\tau) S_{\theta}^{-1}(\tau) \tilde{y}_{\theta}(\tau)].$$

Comparing (21) and (31) it is not hard to show that

$$\mu_{\theta_i}(t) = \frac{1}{t} \log(\mathcal{L}(\theta; Y(t))), \quad (32)$$

from which it follows that

$$\operatorname{argmin}_{\theta_i \in \Theta} \mu_{\theta_i}(t) = \operatorname{argmin}_{\theta_i \in \Theta} t \mu_{\theta_i}(t) = \operatorname{argmax}_{\theta_i \in \Theta} \mathcal{L}(\theta_i; Y(t)). \quad (33)$$

It is further shown in Hassani et al. (2011) that as $t \rightarrow \infty$, the monitoring signal $\mu_{\theta_i}(t)$ converges to Baram index $\Gamma_{\theta_i}^{\theta_*}$ and hence, the estimate in (25) and (26) have similar asymptotic behavior.

3.2 Compact Infinite Parameter Case

Let us investigate the case where Θ is a compact (and convex) set. Assume that θ_* is the true parameter value of the plant. In order to find the maximum likelihood estimate θ one needs to maximize the likelihood function $\mathcal{L}(\theta; Y(t))$ (or minimize $\mathcal{K}(\theta; Y(t))$) over $\theta \in \Theta$, at each sampling time. In Hassani et al. (2013b), a gradient based method is exploited and an algorithm to compute the gradient of $\mathcal{L}(\theta; Y(t))$ with respect to θ is presented. However, in the present paper we use a simpler setup which is based on a bank of N KFs running in parallel to evaluate the value of $\mathcal{L}(\theta; Y(t))$ for N sample points in Θ . After a fixed amount of time Δ a new set of N sample points are selected and a new set of KFs are designed accordingly and the value of $\mathcal{L}(\theta; Y(t))$ is computed for the new sample points in Θ . Under some mild distinguishability condition (see Kashyap (1970)) the maximum likelihood estimator enjoys consistency and one expects that if Δ is selected carefully one can evaluate the value of $\mathcal{L}(\theta; Y(t))$. If we only use the first bank of KFs and we don't re-design the bank of KFs the results coincides with MMA-WF techniques. However, using the new set of KFs enables us to identify the uncertain parameter with higher accuracy. To summarize this section we provide, in the following, a procedure by which the DWF identification is performed.

Algorithm

Initialization: Set $k = 0$ and select N nominal value from the compact parametric uncertainty set and form $\Theta^0 = \{\theta_1^0, \theta_2^0, \dots, \theta_N^0\}$ (see Hassani et al. (2009b) for a performance based selection methodology).

Process:⁵

⁵ The proposed algorithm is straightforward for systems involving a single scalar uncertain real parameter. In the case of two, or more, uncertain parameters the procedure has to be modified. In the

- (1) Design a bank of N KFs based on N plant model associated with the nominal parameter values in Θ^k .
- (2) For Δ seconds run the bank of KFs in parallel and compute $K = \{\mathcal{K}(\theta_1^k; Y(t)), \dots, \mathcal{K}(\theta_N^k; Y(t))\}$.
- (3) Find $\hat{\theta}^k = \underset{\theta_i^k \in \Theta^k}{\operatorname{argmin}} \mathcal{K}(\theta_i^k; Y(t))$.
- (4) Set $k = k + 1$.
- (5) Select N nominal value from the compact parametric uncertainty set and form $\Theta^k = \{\theta_1^k, \theta_2^k, \dots, \theta_N^k\}$ such that $\|\Theta^k\| \leq \|\Theta^{k-1}\|$.
- (6) If $\|\Theta^k\| \leq \delta$ then stop, otherwise go to (1).

4. EXPERIMENTAL RESULTS

The proposed adaptive wave filter was tested using the model vessel *Cybership III*, at the Marine Cybernetic Laboratory (MCLab) of the Department of Marine Technology at the Norwegian University of Science and Technology (NTNU). The performance of maximum likelihood parameter identification was tested under different sea conditions produced by a hydraulic wave maker. Adaptive wave filtering was achieved using the identified DWF and a Kalman wave filter.

4.1 Overview of the *Cybership III*

CyberShip III is a 1:30 scaled model of an offshore vessel operating in the North Sea. Fig. 1 shows the vessel at the basin in the MCLab. See Nguyen et al. (2007); Hassani et al. (2012, 2013c) for details of the main parameters of the model and full scale vessel.



Fig. 1. *Cybership III*.

Cybership III is equipped with two pods located at the aft. A tunnel thruster and an azimuth thruster are installed in the bow.⁶ It has a mass of $m = 75$ (kg), length of $L = 2.27$ (m) and breadth of $B = 0.4$ (m). The internal hardware architecture is controlled by an onboard computer which can communicate with onshore PC through a WLAN. The PC onboard the ship uses the QNX real-time operating system (target PC). The parameter identification, adaptive wave filter, and control systems described before were developed on a PC in the control room (host PC) under Simulink/Opal and downloaded to the target PC using automatic C-code generation and wireless Ethernet. The motion capture unit (MCU), installed in the MCLab, provides Earth-fixed position and heading of the vessel. The MCU consists of onshore 3-cameras mounted on the towing carriage and a marker mounted on the vessel. The cameras emit infrared light and receive the light reflected from a marker on the vessel.

current algorithm we consider the single parametric case. Moreover, for stopping condition we consider $\|\Theta^k\| \leq \delta$ where $\|\Theta\|$ denotes the maximum Euclidian distance among the members of Θ and δ is a predefined limit.

⁶ For technical reasons, in this experiment the tunnel thruster was deactivated.

Due to limited computation power of the PC onboard the ship we implemented the proposed methodology using steady state KFs. We also assumed that the DWFs in surge, sway, and heading are equal, i.e. $\omega_1 = \omega_2 = \omega_3 = \omega$.

To simulate the different sea conditions, a hydraulic wave maker system was used. It consists of a single flap covering the whole breadth of the basin, and a computer controlled motor, moving a flap. The device can produce regular and irregular waves with different spectra. We have used the JONSWAP spectrum to simulate the different sea conditions for our experiment. Fig. 2 shows the results of an experiment where the wave maker system simulates a moderate sea state with $\omega = 0.90$ (rad/sec). The first sub-figure in Fig. 2 shows the wave profile recorded in the basin (two meter in front of the vessel). In this experiment we updated the DWF estimation every 550 seconds. Initially, five KFs were designed based on five different representative values of the uncertain parameter (uniformly distributed in uncertain parameter space, $\{0.6250, 0.8600, 1.0950, 1.3300, 1.5650\}$) and the log-likelihood function of each representative value (given by (21)) was evaluated. At time $t = 550$ (sec) the KF tuned for $\omega = 1.0950$ (rad/sec) had the maximum log-likelihood value. At this point, a new bank of KFs were designed based on a new set of representative DWFs $\{0.7817, 0.9383, 1.0950, 1.2517, 1.4083\}$ and the log-likelihood function was evaluated for the mentioned set. At $t = 1100$ (sec) the DWF estimation was updated to $\omega = 0.9383$ (rad/sec) (that has the maximum log-likelihood function). The fifth sub-figure in Fig. 2 represents the estimated DWF and Fig. 3 shows the log-likelihood functions. The second, third and fourth sub-figures in Fig. 2 show the time evolution of the positions and heading of the vessel. It can be seen that the DWF estimation converged to $\omega = 1.0255$ (rad/sec) after five estimation steps. This is different from the set value of the wave maker; later, we estimated the power spectral density of time series of wave elevation and we found that a more accurate DWF value was $\omega = 0.96$ (rad/sec). We hypothesize that the small bias in the estimation is due to a) the simplified model of plant used for identification, b) the assumption of equal DWFs in surge, sway, and heading, and c) the tuning of the disturbance covariances in the KFs.⁷

5. CONCLUSIONS

The problem of parameter identification for adaptive WF in DP of marine vessels was addressed in a systematic way for discrete-time, linear, time-invariant MIMO plants with parameter uncertainty maximum likelihood methodology. To this effect, the maximum likelihood parameter identification was re-visited and the link between the proposed identification methodology and the one in Multiple Model Adaptive Estimation was investigated. The results were experimentally verified by model testing a DP operated ship, the *Cybership III*, under simulated sea condition in a towing tank. The experimental data confirms that the method developed holds promise for practical applications. Future work will include the application of the method developed to time-varying operational conditions, from calm to extreme seas.

ACKNOWLEDGEMENTS

We thank our colleagues A. Pedro Aguiar, J. Hespanha and Michael Athans for many discussions on adaptive

⁷ We should stress that we have tuned the algorithm during a few tests and Fig. 2 shows the final tuned system.

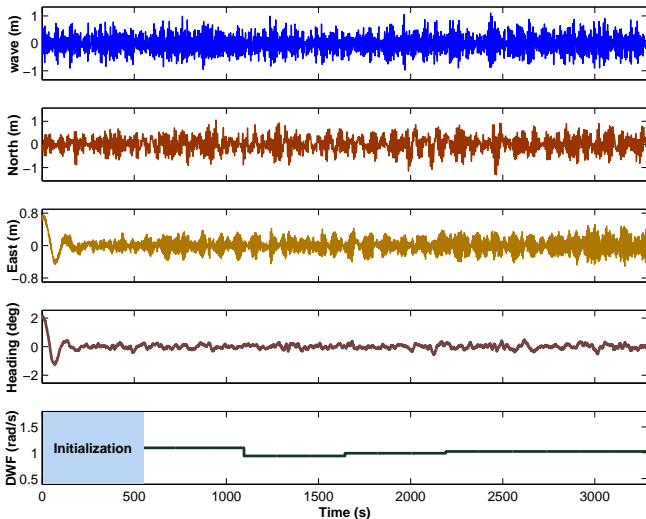


Fig. 2. Experimental results: evolution of the wave profile, the position and heading of the vessel, and the DWF estimation in moderate sea state.

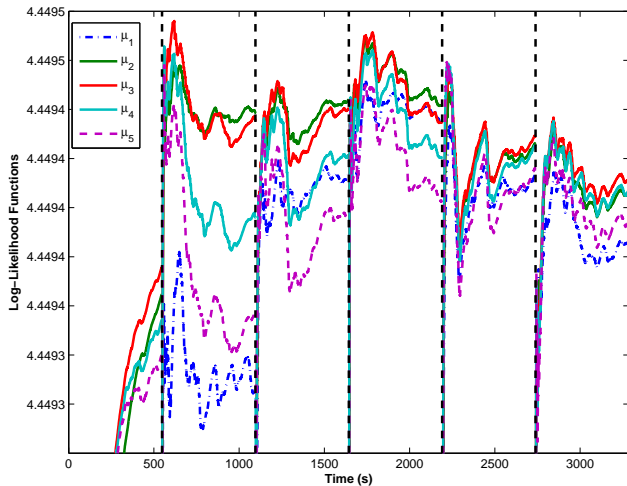


Fig. 3. Experimental results: evolution of the log-likelihood functions; every 550 seconds a new set of KFs are designed to evaluate the log-likelihood function for a new set of uncertain parameters (DWF).

estimation and control. We would also like to thank T. Wahl, Øyvind Smogeli, M. Etemaddar, E. Peymani, M. Shapouri, and B. Ommani for their generous assistance during the model tests at MCLab.

REFERENCES

- Anderson, B.D.O. and Moore, J.B. (1979). *Optimal Filtering*. Prentice-Hall, New Jersey, USA.
- Balchen, J., Jenssen, N., and Sælid, S. (1976). Dynamic positioning using Kalman filtering and optimal control theory. In *the IFAC/IFIP Symposium On Automation in Offshore Oil Field Operation*, 183–186. Bergen, Norway.
- Baram, Y. and Sandell, N. (1978). An information theoretic approach to dynamical systems modeling and identification. *IEEE Trans. on Automat. Contr.*, 23, 61–66.
- Fossen, T.I. (2011). *Handbook of Marine Craft Hydrodynamics and Motion Control*. John Wiley & Sons. Ltd, Chichester, UK.
- Fossen, T.I. and Strand, J.P. (1999). Passive nonlinear observer design for ships using lyapunov methods: Full-scale experiments with a supply vessel. *Automatica*, 35, 3–16.
- Grøvlen, Å. and Fossen, T.I. (1996). Nonlinear control of dynamic positioned ships using only position feedback: An observer backstepping approach. In *Proc. IEEE Conference on Decision and Control (CDC'96)*. Kobe, Japan.
- Hassani, V., Aguiar, A.P., Athans, M., and Pascoal, A.M. (2009a). Multiple model adaptive estimation and model identification using a minimum energy criterion. In *Proc. ACC'09 - American Control Conference*. St. Louis, Missouri, USA.
- Hassani, V., Aguiar, A.P., Pascoal, A.M., and Athans, M. (2009b). A performance based model-set design strategy for multiple model adaptive estimation. In *ECC'09 - European Control Conference*. Budapest, Hungary.
- Hassani, V., Hespanha, J., Athans, M., and Pascoal, A.M. (2011). Stability analysis of robust multiple model adaptive control. In *Proc. of The 18th IFAC World Congress*. Milan, Italy.
- Hassani, V., Pascoal, A.M., and Aguiar, A.P. (2013a). Multiple model adaptive estimation for open loop unstable plants. In *Proc. ECC'13 - European Control Conference*. Zurich, Switzerland.
- Hassani, V., Pascoal, A.M., and Sørensen, A.J. (2013b). A novel methodology for adaptive wave filtering of marine vessels: Theory and experiments. In *Proc. IEEE Conference on Decision and Control (CDC'13)*. Florence, Italy.
- Hassani, V., Sørensen, A.J., and Pascoal, A.M. (2013c). A novel methodology for robust dynamic positioning of marine vessels: Theory and experiments. In *Proc. ACC'13 - American Control Conference*. Washington, DC, USA.
- Hassani, V., Sørensen, A.J., Pascoal, A.M., and Aguiar, A.P. (2012). Multiple model adaptive wave filtering for dynamic positioning of marine vessels. In *Proc. ACC'12 - American Control Conference*. Montreal, Canada.
- Kashyap, R. (1970). Maximum likelihood identification of stochastic linear systems. *IEEE Transactions on Automatic Control*, 15(1), 25–34.
- Nguyen, T.D., Sørensen, A.J., and Quek, S.T. (2007). Design of hybrid controller for dynamic positioning from calm to extreme sea conditions. *Automatica*, 43(5), 768–785.
- Price, W.G. and Bishop, R.E.D. (1974). *Probabilistic Theory of Ship Dynamics*. Chapman and Hall, London, UK.
- Sælid, S., Jenssen, N.A., and Balchen, J. (1983). Design and analysis of a dynamic positioning system based on Kalman filtering and optimal control. *IEEE Transactions on Automatic Control*, 28(3), 331–339.
- Sørensen, A.J. (2011). A survey of dynamic positioning control systems. *Annual Reviews in Control*, 35, 123–136.
- Sørensen, A.J., Sagatun, S.I., and Fossen, T.I. (1996). Design of a dynamic positioning system using model-based control. *Journal of Control Engineering Practice*, 4(3), 359–368.
- Strand, J.P. and Fossen, T.I. (1999). Nonlinear passive observer for ships with adaptive wave filtering. *New Directions in Nonlinear Observer Design (H. Nijmeijer and T. I. Fossen, Eds.)*, Springer-Verlag London Ltd., 113–134.
- Torsetnes, G., Jouffroy, J., and Fossen, T.I. (2004). Non-linear dynamic positioning of ships with gain-scheduled wave filtering. In *Proc. IEEE Conference on Decision and Control (CDC'04)*. Paradise Island, Bahamas.